Control of Intramolecular Electron Transfer by Protonation: Oligomers of Ruthenium Porphyrins Bridged by 4,4'-Azopyridine

Valérie Marvaud and Jean-Pierre Launay*

Molecular Electronics Group, CEMES/LOE, CNRS, 29 rue Jeanne Marvig, 31055 Toulouse Cedex, France

Received August 11, 1992

The association of pentaammineruthenium(II) with the reducible ligand 4,4'-azopyridine leads to a pH-induced redox reaction in which ruthenium is oxidized to the III state, while 4,4'-azopyridine is reduced to hydrazopyridine. In this process, the conjugated ligand is transformed in a nonconjugated one, with loss of its intramolecular electron-transfer properties. In order to exploit this *control of an intramolecular electron transfer by a protonation process*, we have prepared "shish kebab" oligomers by first inserting a ruthenium chloro carbonyl complex in tetrakis(3,5-di-*tert*-butyl-4-hydroxyphenyl)porphyrin. The resulting Ru(CO)(porphyrin) complex is photochemically decarbonylated in the presence of bridging ligands (4,4'-azopyridine or pyrazine). Oligomers are thus obtained, which can be oxidized by iodine, giving rise to intervalence transitions between ruthenium(II) and -(III) in the near-infrared. This provides a convenient way to monitor electron transfer along the oligomer chain. In the case of 4,4'-azopyridine, the pH-induced redox reaction is again observed. Starting from a homovalent ruthenium(II) chain, this gives the possibility to switch "on" or "off" the intervalence transition by a protonation/deprotonation reaction.

Introduction

The synthesis of molecular switches appears to be a major challenge in molecular electronics. From the point of view of synthetic chemistry, a molecular switch can be viewed as a structure in which two redox sites are connected by a central unit which can adopt two possible states, one allowing the electron transfer between the outer redox sites and one blocking it. At present two general switching possibilities have been experimentally explored, corresponding to the perturbation of the central unit by a photophysical[1] or a chemical[2] effect.

Chemical perturbation offers certain advantages; in particular it can be made reversible and does not need sophisticated equipment to be activated. Among the possible chemical reactions, protonation is one of the simplest and could be, if necessary, coupled with other physical processes such as electrochemistry or photochemistry to manipulate the proton concentration. Since protons are highly mobile in protonic solvents, they could play the role of mediators between the different molecules to couple.

Several examples in which an intramolecular electron transfer is controlled by a protonation/deprotonation state are presently known. As discussed elsewhere,[3] protonation can be considered as a way to polarize (or even remove) π electrons. Thus, in 1976, Krentzien and Taube[4] described the interesting properties of *tert*-butylmalonitrile as bridging ligand. A strong increase in metal-metal interaction was observed upon deprotonation. More recently, Haasnoot et al.[5] reported the interesting properties of binuclear ruthenium complexes bridged by 3,5-bis(pyridin-2-yl)-1,2,4-triazole. The clearest examples has been published quite recently by Haga et al.:[6] By a detailed study of intervalence transitions through a protonated and a deprotonated form of the bridging ligand 2,2'-bis(2-pyridyl)bibenzimidazole, they have been able to show the influence of protons on electron transfer. Finally, it is useful to recall the fascinating properties of polyaniline, the conductivity of which can change by several orders of magnitude according to the protonation state.[7]

For our part we have undertaken a study of electron transfer through the bridging ligand 4,4'-azopyridine (abbreviated in the following as azpy). The binuclear complex with pentaammineruthenium has been used to probe the electron-transfer properties. We have found that the following proton-induced redox reaction occurs:[8]

$$[(NH_3)_5Ru^{II}\text{-}L\text{-}Ru^{II}(NH_3)_5]^{4+} + 2H^+ \rightarrow [(NH_3)_5Ru^{III}\text{-}LH_2\text{-}Ru^{III}(NH_3)_5]^{6+}$$

Here L = 4,4'-azopyridine and LH_2 = 1,2-bis(4-pyridyl)-hydrazine. This reaction can be considered as the reduction of the azo group by two protons (provided by the medium) and two electrons (taken from the ruthenium(II) sites). This changes the electronic structure of the bridging ligand,[8] and it can be shown in a qualitative way that the electronic interaction through LH_2 is strongly reduced with respect to L.

In order to fully exploit this effect, it would be better to use an extended polymeric system so that the electron-transfer process could be monitored ultimately by a macroscopic parameter such as resistance. Fortunately such systems have been already described by the groups of Hanack[9] and Collman:[10] They exhibit a "shish kebab" structure built from metal macrocycles (macrocycle = porphyrin or phthalocyanin) in which the two axial positions of the metal are used for coordination with a bridging ligand. Interestingly, this particular structure allows the use of the same ligands as for binuclear complexes.

In the present paper we describe new results obtained with polymers (in fact oligomers) of ruthenium porphyrin bridged by

* To whom correspondence should be addressed.

(1) Launay, J.-P.; Joachim, C. *J. Chim. Phys. Physicochim. Biol.* **1988**, *85*, 1135.
(2) Gourdon, A. *New. J. Chem.* **1992**, *16*, 953.
(3) Joachim, C.; Launay, J.-P. *J. Mol. Electron.* **1990**, *6*, 37.
(4) Krentzien, H.; Taube, H. *J. Am. Chem. Soc.* **1976**, *98*, 6379. Krentzien, H.; Taube, H. *Inorg. Chem.* **1982**, *21*, 4001.
(5) Hage, R.; Dijkhuis, A. H. J.; Haasnoot, J. G.; Prins, R.; Reedijk, J.; Buchanan, B. E.; Vos, J. G. *Inorg. Chem.* **1988**, *27*, 2185.
(6) Haga, M.-a.; Ano, T.-a.; Kano, K.; Yamabe, S. *Inorg. Chem.* **1991**, *30*, 3843.
(7) Travers, J. P.; Chroboczek, J.; Devreux, F.; Genoud, F.; Nechtschein, M.; Syed, A.; Genies, E. M.; Tsintavis, C. *Mol. Cryst. Liq. Cryst.* **1985**, *121*, 195.
(8) Launay, J.-P.; Tourrel-Pagis, M.; Lipskier, J.-F.; Marvaud, V.; Joachim. C. *Inorg. Chem.* **1991**, *30*, 1033.
(9) Kobel, W.; Hanack, M. *Inorg. Chem.* **1986**, *25*, 103.
(10) Collman, J. P.; Mc Devitt, J. T.; Leidner, C. R.; Yee, G. T.; Torrance, J. B.; Little, W. A. *J. Am. Chem. Soc.* **1987**, *109*, 4606.

0020-1669/93/1332-1376$04.00/0

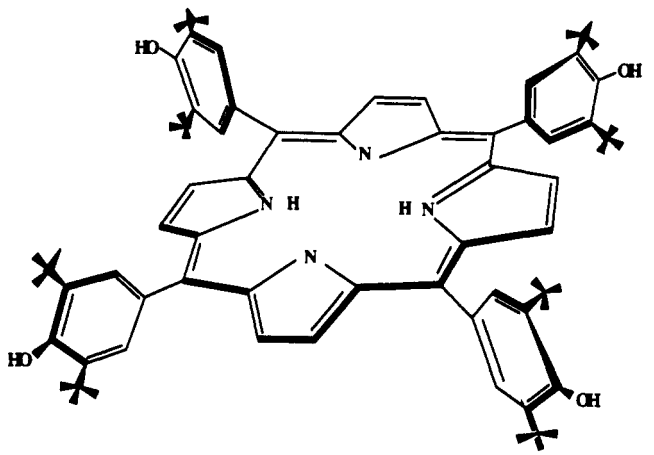

Figure 1. Structure of (3,5-di-*tert*-butyl-4-hydroxyphenyl)porphyrin.

pyrazine (abbreviated as pyz) and 4,4′-azopyridine. We have used tetrakis(3,5-di-*tert*-butyl-4-hydroxyphenyl)porphyrin (abbreviated as TBP) first described by Milgrom[11] (see Figure 1), which offers several specific advantages over more common porphyrins such as octaethylporphyrin or tetraphenylporphyrin; i.e., the synthesis is easy, the solubility is rather good, and the presence of phenol functions gives rise to a rich redox chemistry (this last aspect is potentially interesting for future developments but has not been exploited here).

Experimental Section

4,4′-Azopyridine was prepared according to a procedure already described.[8] Solvents were analytical grade, except for irradiations where spectrophotometric grade was used. UV–vis–near-IR spectra were recorded with a Beckman 5240 or a Shimadzu UV-3101 PC spectrophotometer. IR spectra were recorded in KBr pellets with a Perkin-Elmer 457 or a 1725 X (FTIR). NMR spectra were recorded with a Bruker WM 250 or a Bruker FT NMR 200-AF spectrometer. The proton nomenclature and assignment for some compounds are summarized on Figure 2. Cyclic voltammetry curves were recorded with an Electromat 2000 system from ISMP Technologie (Labège, Haute Garonne, France), using a platinum wire as working electrode, CH_2Cl_2 (HPLC grade) as solvent, and tetrabutylammonium tetrafluoroborate as supporting electrolyte. The scan rate was 0.1 V s^{-1}, and potentials were measured using a saturated calomel electrode (SCE) with a double frit system. The exploration was performed from 0 to −1.5 V for cathodic peaks and from 0 to 1.8 V for anodic peaks.

Tetrakis(3,5-di-*tert*-butyl-4-hydroxyphenyl)porphyrin, (H_2TBP). We have followed the preparation from 3,5-di-*tert*-butyl-4-hydroxybenzaldehyde and pyrrole described by Milgrom.[11]

Anal. Calcd for $C_{76}N_4O_4H_{94}$: C, 80.95; H, 8.40; N, 4.97. Found: C, 80.78; H, 8.43; N, 4.68. UV–vis in ethanol (λ_{max}, nm): 420 (Soret), 523, 561, 596, 653. NMR ($CDCl_3$, 250 MHz): t-bu 1.65 (s), H_{pyrr} 8.96 (s), H_o 8.07 (s), H_{OH} 5.55 (s), H_{NH} −2.61 (s).

Carbonyl(ethanol)(tetrakis(3,5-di-*tert*-butyl-4-hydroxyphenyl)porphyrinato)ruthenium(II), [Ru(TBP)CO(EtOH)]. Using the method of Collman et al. for tetraphenylporphyrin,[12] 1.5 g of hydrated $RuCl_3$ (5 mmol) was dissolved in 60 mL of diethylene glycol monomethyl ether (alternate name: 2-(2-methoxyethoxy)ethanol) (Merck) and heated to 160 °C while bubbling CO. After 4 h, the limpid yellow solution was cooled and added dropwise to a boiling solution of H_2TBP (3 g, 2.6 mmol) in 100 mL of diethylene glycol monomethyl ether under nitrogen. The mixture was refluxed under nitrogen until disappearance of the visible bands of H_2TBP (typically 2 h). The dark red solution was then cooled and filtrated (a ruthenium mirror usually formed on the flask wall). The filtrate was then precipitated by 400 mL of an aqueous NaCl solution (2 M) and stirred for 2 h. The mixture was filtrated on Celite, washed thoroughly with water, and dried under vacuum. Extraction from Celite was performed with an $EtOH/CH_2Cl_2$ mixture (5/95). After solvent evaporation, the solid residue was dissolved in toluene and chromatographed on SiO_2. The carbonyl complex was finally recrystallized from ethanol. Yield: 2.2 g (1.7 mmol, 64%).

(11) Milgrom, L. *Tetrahedron* **1983**, *39*, 3895.
(12) Collman, J. P.; Barnes, C. E.; Swepston, P. N.; Ibers, J. A. *J. Am. Chem. Soc.* **1984**, *106*, 3500.

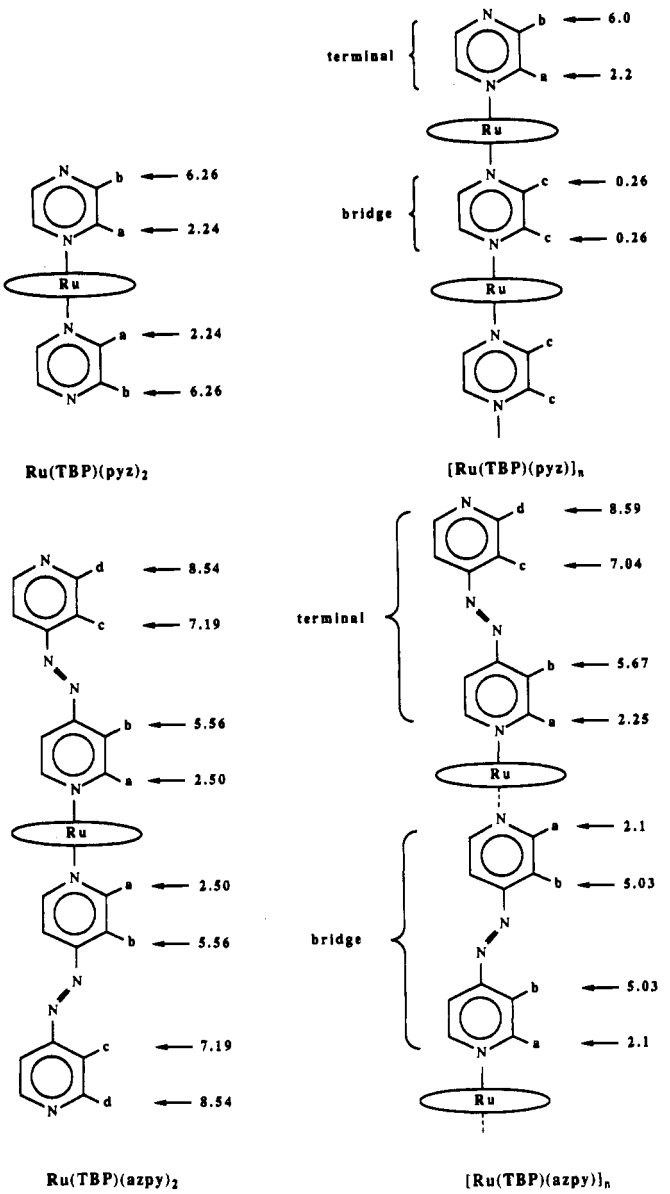

Figure 2. Proton nomenclature for $[Ru(TBP)(pyz)_2]$, $[Ru(TBP)(pyz)]_n$, $[Ru(TBP)(azpy)_2]$, and $[Ru(TBP)(azpy)]_n$.

Anal. Calcd for $C_{79}N_4O_6H_{98}Ru$: C, 72.95; H, 7.59; N, 4.31. Found: C, 73.16; H, 7.81; N, 4.07. UV–vis in ethanol (λ_{max}, nm): 417 (Soret), 531, 567. IR (ν, cm^{-1}) in KBr: 1935 (CO). NMR ($CDCl_3$, 250 MHz): t-bu 1.63 (s), H_{pyrr} 8.8 (s), H_o 7.95 (1.9 Hz d), H'_o 8.03 (1.9 Hz d), H_{OH} 5.5 (s).

Decarbonylation Procedure. In a typical experiment, 400 mg (0.3 mmol) of [Ru(TBP)CO(EtOH)] was dissolved in 800 mL of absolute ethanol and thoroughly degassed by bubbling argon. A photochemical reactor consisting of a medium-pressure mercury vapor lamp (Hanovia 679 A) surrounded by a water jacket was immersed in the solution. Irradiation was performed for 2 h with argon bubbling to evacuate CO. UV–vis showed the complete disappearance of the 531- and 567-nm bands. The solution then contained $[Ru(TBP)(EtOH)_2]$, which was used in situ. UV–vis/near-IR (λ_{max}, nm): 415 (Soret), 523.

Diacetonitrile(tetrakis(3,5-di-*tert*-butyl-4-hydroxyphenyl)porphyrinato)ruthenium(II), [Ru(TBP)(CH_3CN)$_2$]. The same procedure as above was used, with acetonitrile (spectrophotometric grade) as solvent. After irradiation, the solvent was evaporated and the residue dried under vacuum giving a brown powder. Yield: 95%.

Anal. Calcd for $C_{80}N_6O_4H_{98}Ru + 4H_2O$: C, 69.58; H, 7.73; N, 6.08. Found: C, 69.55; H, 7.53; N, 5.86. UV–vis in acetonitrile (λ_{max}, nm): 419 (Soret), 507. IR (ν, cm^{-1}) in KBr: 2240 (w) (CH_3CN), 3600 (OH with H bond). NMR ($CDCl_3$, 250 MHz): t-bu 1.70 (s), H_{pyrr} 8.74 (s), H_o 7.95 (s), H_{OH} 5.48 (s).

Dipyrazine(tetrakis(3,5-di-*tert*-butyl-4-hydroxyphenyl)porphyrinato)ruthenium(II), [Ru(TBP)(pyrazine)$_2$]. A 400-mg amount of [Ru(TBP)-CO(EtOH)] (0.3 mmol) was dissolved in 800 mL of absolute ethanol and

irradiated under argon until disappearance of Ru(TBP)CO. Then 1.2 g of pyrazine (15 mmol) dissolved in the minimum volume of ethanol was added and the irradiation was resumed for 1 h 30 min under strict argon protection. The solvent was then evaporated, and the red product was chromatographed on SiO_2 with CH_2Cl_2 as eluant.

Anal. Calcd for $C_{84}N_8O_4H_{100}Ru$: C, 72.75; H, 7.27; N, 8.08. Found: C, 72.55; H, 7.52; N, 8.23. UV–vis in ethanol (λ_{max}, nm): 258, 278 (pyrazine bands), 420 (Soret), 508, 565. IR (ν, cm^{-1}) in KBr: 1579 (s) (terminal pyrazine). NMR ($CDCl_3$, 200 MHz): t-bu 1.59 (s), H_{pyrr} 8.46 (s), H_o 7.84 (s), H_{OH} 5.43 (s), $H_{a,pyz}$ 2.24 (3.2 Hz d), $H_{b,pyz}$ 6.26 (3.2 Hz d).

Bis(4,4′-azopyridine)(tetrakis(3,5-di-*tert*-butyl-4-hydroxyphenyl)porphyrinato)ruthenium(II), [Ru(TBP)(azopyridine)$_2$]. A 260-mg amount of [Ru(TBP)CO(EtOH)] (0.2 mmol) dissolved in 800 mL of ethanol was irradiated as described above. After complete disappearance of the UV–vis bands of the carbonyl complex, the irradiation was stopped and a solution of 150 mg (0.8 mmol) of 4,4′-azopyridine in 20 mL of ethanol was added. Irradiation was resumed for 15 min under argon. The crude product obtained after solvent evaporation was dissolved in 5 mL of EtOH and precipitated by pouring in 500 mL of a 1 M NaCl solution. It was then filtrated on Celite, extracted with ethanol, and chromatographed on SiO_2 with CH_2Cl_2 as eluant. Solvent evaporation yielded a dark green powder which could be recrystallized in EtOH. Yield: 240 mg (0.15 mmol, 75%).

Anal. Calcd for $C_{96}N_{12}O_4H_{108}Ru$ + 6EtOH: C, 69.34; H, 7.70; N, 8.98. Found: C, 69.40; H, 8.01; N, 9.15. UV–vis/near-IR in ethanol (λ_{max}, nm): 282 (azopyridine), 420 (Soret), 506, 825. NMR ($CDCl_3$, 200 MHz): t-bu 1.58 (s), H_{pyrr} 8.43 (s), H_o 7.86 (s), H_{OH} 5.41 (s), $H_{a,azpy}$ 2.50 (5.5 Hz d), $H_{b,azpy}$ 5.56 (5.5 Hz d), $H_{c,azpy}$ 7.19 (4.6 Hz d), $H_{d,azpy}$ 8.54 (4.6 Hz d).

(μ-Pyrazine)(tetrakis(3,5-di-*tert*-butyl-4-hydroxyphenyl)porphyrinato)ruthenium(II), [Ru(TBP)(pyrazine)]$_n$. A 50-mg amount of [Ru(TBP)CO(EtOH)] (0.038 mmol) was dissolved in 100 mL of deaerated ethanol and irradiated in a quartz vessel placed near the Hanovia lamp. To increase the efficiency, an aluminum foil was wrapped around the lamp and vessel. After 2 h, the complete transformation was checked by UV–vis spectroscopy. The volume was then reduced to $^1/_4$ by pumping under vacuum, and 3.2 mg of pyrazine (0.038 mmol) dissolved in 1 mL of ethanol was added. Irradiation was resumed for 10 min under argon protection. The solvent was then evaporated slowly on a vacuum line, and the dark green solid residue was washed with ethanol.

Anal. Calcd for $C_{80}N_6O_4H_{96}Ru$: C, 73.56; H, 7.36; N, 6.44. Found: C, 73.21; H, 7.29; N, 6.64. UV–vis/near-IR in ethanol (λ_{max}, nm): 271 (pyrazine), 411 (Soret), 511, 744. IR (ν, cm^{-1}) in KBr: 1581 (w) (terminal pyrazine). NMR ($CDCl_3$, 250 MHz): t-bu 1.27 (m), $H_{pyrr,term}$ 7.90 (w), $H_{pyrr,inner}$ 7.45 (w), H_o 7.05 (w), H_{OH} 5.27 (w), $H_{a,pyz,term}$ 2.2 (w), $H_{b,pyz,term}$ 6.0 (w), $H_{pyz,bridg}$ 0.26 (w) (w = wide peaks).

(μ-4,4′-Azopyridine)(tetrakis(3,5-di-*tert*-butyl-4-hydroxyphenyl)porphyrinato)ruthenium(II), [Ru(TBP)(azopyridine)]$_n$. The same procedure as above was used, with 50 mg of [Ru(TBP)CO(EtOH)] (0.038 mmol) in 150 mL of deaerated ethanol and 7.1 mg of 4,4′-azopyridine (0.038 mmol) dissolved in 1 mL of deaerated ethanol. Contrary to the previous case, a precipitate formed during the reaction. It was filtrated out, washed with ethanol and hexane, and dried. A violet microcrystalline powder was obtained (37.6 mg, yield 69%).

Anal. Calcd for $C_{86}N_8O_4H_{100}Ru$ + 2EtOH + $2H_2O$: C, 70.23; H, 7.59; N, 7.28. Found: C, 70.13; H, 7.67; N, 7.33. UV–vis/near-IR in $CHCl_3$ (λ_{max}, nm): 282 (azopyridine), 420 (Soret), 508, 966. NMR ($CDCl_3$, 250 MHz): t-bu 1.49 (m), H_{pyrr} 8.22 (w), H_o 7.53 (w), H_{OH} 5.33 (w), bridging azpy, $H_{a,azpy}$ 2.1 (w), $H_{b,azpy}$ 5.03 (w); terminal azpy, $H_{a,azpy}$ 2.25 (d), $H_{b,azpy}$ 5.67 (d), $H_{c,azpy}$ 7.04 (d), $H_{d,azpy}$ 8.59 (d) (w = wide peaks). Additional peaks due to included ethanol and water were also observed.

Oxidation Experiments. Oxidation experiments necessary to generate the mixed-valence forms were performed by adding aliquots of a solution of iodine in chloroform. Two kinds of experiments were usually performed: a titration in "diluted" solutions to see the decrease of the ruthenium-to-axial-ligand charge transfer and a titration in "concentrated" solution to observe intervalence transitions. Typical concentrations were in the first case 2×10^{-4} mol·L^{-1} (in monomeric units) for the oligomer and 4×10^{-3} mol·L^{-1} for the iodine solutions and in the second case 10^{-3} mol·L^{-1} and 1.6×10^{-2} mol·L^{-1}, respectively.

Generation of the Oligomer Bridged by 1,2-Bis(4-pyridyl)hydrazine. The azopyridine oligomer (3 mL of a 10^{-3} M solution in chloroform) was acidified by bubbling gaseous hydrogen chloride until disappearance of the metal-to-axial charge-transfer bands, and then sodium borohydride (3 mg, i.e. 0.078 mmol) was added to the solution.

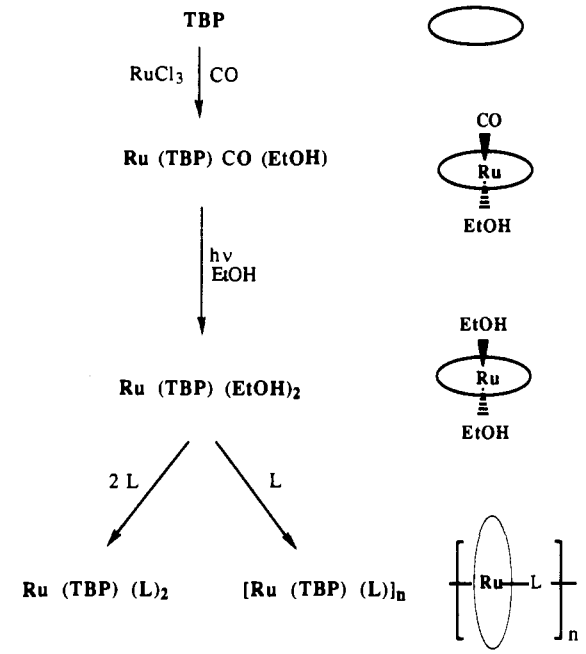

Figure 3. General synthetic scheme.

Results and Discussion

Ruthenium Chemistry. The general synthetic scheme leading to oligomers is summarized on Figure 3. Insertion of ruthenium has been performed using the general method described by Collman,[12] i.e. heating to reflux in diethylene glycol monomethyl ether a mixture of porphyrin and of a chloro carbonyl complex obtained from $RuCl_3$ and CO. This yields [Ru(TBP)CO(S)] (S = solvent molecule) which is isolated and purified by chromatography. Decarbonylation proved to be the most difficult step. We found that the best procedure was to irradiate a solution of the carbonyl complex for 2 h with a mercury vapor lamp, while bubbling argon to remove carbon monoxide. When irradiation is performed in acetonitrile, a coordinating solvent, the [Ru(TBP)$(CH_3CN)_2$] complex is formed, which can be isolated in the solid state. In ethanol, a weakly coordinating solvent, the analogous [Ru(TBP)$(EtOH)_2$] is certainly formed, but it is much more reactive, so that it must be used in situ. Its formation is however strongly supported by the analogy of its UV–visible spectrum with the one of [Ru(TBP)$(CH_3CN)_2$] and by its subsequent reactivity.

Addition of a bridging ligand to a photolyzed solution of [Ru(TBP)CO(EtOH)] in ethanol, eventually followed by an additional photolysis, gave two kinds of complexes: (i) With an excess of the bridging ligand, we obtain monometallic complexes of the type [Ru(TBP)$(L)_2$] which can be used as a model of the constitutive unit of the oligomer. (ii) With a stoichiometric ratio of 1 ligand for 1 [Ru(TBP)$(EtOH)_2$], we obtain oligomers of general formula [Ru(TBP)$(L)]_n$. Both kinds of compounds have been prepared with L = pyrazine and L = azopyridine and have been characterized by microanalysis, UV–vis spectroscopy, IR spectroscopy, and NMR.

The NMR spectra give some interesting indications on the porphyrin cycle, the axial ligands, and their mutual interactions. Thus, in [Ru(TBP)CO(EtOH)], the aromatic protons of the (3,5-di-*tert*-butyl-4-hydroxyphenyl) groups, denoted as H_o and H'_o, are nonequivalent, showing that there is no free rotation of the phenyl rings (at least in the NMR time scale), due to steric crowding. In the [Ru(TBP)$(L)_2$] complexes, they become again equivalent because the axial ligands are identical. Regarding the axial ligands, they undergo the influence of the ring currents induced in the porphyrin. Thus in the [Ru(TBP)$(pyz)_2$] complex, the protons adjacent to the coordinated nitrogen are strongly shielded with respect to normal pyrazine protons (8.5 ppm) and appear at 2.24 ppm. In the [Ru(TBP)$(pyz)]_n$ oligomer, since the

bridging ligand is short, all pyrazine undergo the influence of *two* porphyrin rings (at least for the bridging pyrazine; see below). This gives them an unusual 0.26 ppm chemical shift.

For the [Ru(TBP)(azpy)$_2$] complex, the azpy ligand exhibits four types of protons, with chemical shifts ranging from 2.5 to 8.54 ppm; these shifts can be directly correlated with the distance from the porphyrin ring (see Figure 2). For comparison, the free azpy ligand gives peaks at 8.85 and 7.7 ppm (doublets of doublets).

In the [Ru(TBP)(azpy)]$_n$ oligomer, again the influences of two porphyrin rings add at the bridging azpy, pushing the signals to 5.03 and 2.1 ppm. These simple considerations allow the distinction between bridging and terminal azopyridine to be made (see below).

The condensation degree n of the oligomers has been estimated by spectroscopic methods. For the pyrazine-bridged oligomers, one uses the fact that the pyrazine symmetrical "breathing" mode at 1581 cm^{-1} is normally forbidden but can appear if the symmetry of the molecule is lost by coordination on one nitrogen only. Thus, following Collman et al.,[10] the intensity ratio of this band between [Ru(TBP)(pyrazine)]$_n$ and [Ru(TBP)(pyrazine)$_2$] can be used to estimate the degree of polymerization, after a normalization of the spectra, using a porphyrin band as reference. We have thus found $n = 5 \pm 1$. This estimation relies on the assumption that all chains are capped, i.e. terminated by a ...(pyz)Ru(TBP)-(pyz) moiety, as also assumed in the early work by Collman et al.[10] This is certainly the case because the reaction is performed under stoichiometric conditions (or eventually with a very small excess of pyrazine), and it can be checked by NMR that no free pyrazine remains. In addition, the porphyrin H_o peaks appear as singlets, which shows that the porphyrin cycles are surrounded by two axial ligands (in the reverse case, two peaks would be observed as in [Ru(TBP)CO(EtOH)]).

Another independent estimation of the condensation degree is possible by NMR, using the peaks at 0.26 and 6.0 ppm which correspond respectively to bridging and terminal pyrazine. We have thus found $n = 6$, in good agreement with the IR estimation.

For the azopyridine oligomer, no IR data can be used: we have carefully compared the spectra of free azpy and azpy complexed in [Ru(TBP)(azpy)$_2$] but no difference in the azopyridine band could be found, showing that the spectra of bridging and terminal azpy are qualitatively the same. NMR makes however a distinction between bridging and terminal azopyridine (see figure). Thus by integration of the 5.03 and the 5.67 ppm peaks, we have been able to evaluate the ratio between bridging and terminal azpy, which gave $n = 13 \pm 1$.

Thus, the obtained compounds are more properly qualified as oligomers of ruthenium porphyrins. For this reason, we have not attempted conductivity measurements, which would be most likely dominated by intermolecular effects. Rather, we have tried to characterize the electron delocalization by spectroscopic studies.

Metal-to-Axial Ligand Charge-Transfer Bands. The UV–visible absorption spectra of all compounds show the intense Soret band of the porphyrin near 415 nm. Less intense Q bands are also observed, which can be used to follow the different synthesis steps. Thus free TBP exhibits four Q bands while [Ru(TBP)-CO(S)] exhibits two bands as usual for a metalated porphyrin;[13] moreover, we have noticed that the more symmetrical complexes [Ru(TBP)(L)$_2$] and [Ru(TBP)(L)]$_n$ exhibit just one band in the Q region. In addition to these bands, we have found lower energy bands (see Table I) which are dependent upon the ligand nature and exhibit solvatochromism. Thus in the case of [Ru(TBP)-(azpy)$_2$] for which these bands are particularly well resolved with respect to the porphyrin bands, one observes λ_{max} = 804, 818, and 848 nm in acetone, dichloromethane, and ethanol, respectively. This behavior is typical of *metal-to-axial ligand charge-transfer bands*. The strongest argument for such an assignment is the correlation between the band energy and the reducibility of the ligand. Thus, when the pyrazine and azopyridine complexes are compared, the lowest energy is observed with the more reducible azopyridine ligand (see Table I and Figure 4). Incidentally, the existence of these bands has been already postulated but their actual assignment remained doubtful.[14] In the present complexes where the bands are intense and well separated, the assignment seems to rely on firmer grounds.

Table I. Position and Apparent Coefficients of the Ruthenium-to-Axial Ligand Charge-Transfer Bands (pyz = Pyrazine; azpy = 4,4′-Azopyridine)[a]

compd	λ, nm (ε, mol^{-1}·L·cm^{-1})
[Ru(TBP)(pyz)$_2$]	565 (4500)
[Ru(TBP)(pyz)]$_n$	744 (12 000)
[Ru(TBP)(azpy)$_2$]	825 (5700)
[Ru(TBP)(azpy)]$_n$	966 (9500)

[a] Extinction coefficients are relative to Ru(TBP) units. n is the condensation degree of the oligomers (ca. 5 for pyrazine and ca. 13 for azopyridine).

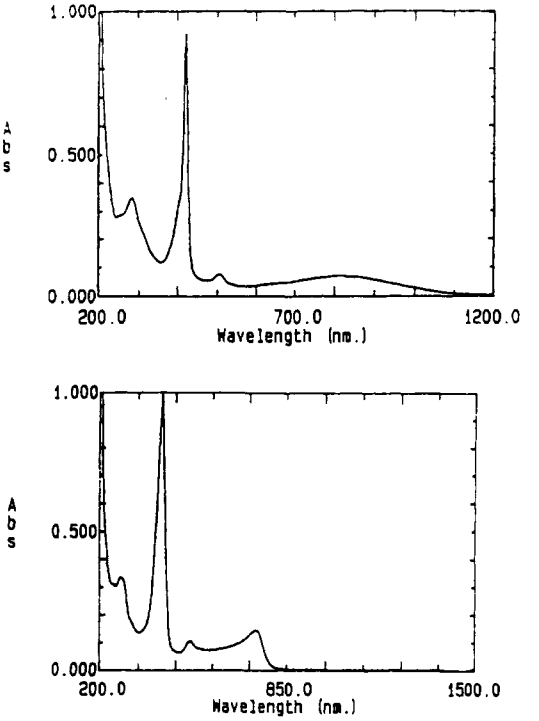

Figure 4. Electronic spectra in ethanol (1-cm path length): (a, top) [Ru(TBP)(azpy)$_2$] ($C = 1.25 \times 10^{-5}$ M); (b, bottom) [Ru(TBP)(pyz)]$_n$ ($C = 1.2 \times 10^{-5}$ M).

An interesting comparison can be made between the mononuclear [Ru(TBP)(L)$_2$] species and the oligomers [Ru(TBP)-(L)]$_n$. Thus the energy of the bands is decreased upon polymerization (see Table I). At the same time, the extinction coefficient (calculated in all cases with respect to mononuclear units) increases markedly, despite the fact that the oligomer contains only one L per monomeric unit, instead of two in [Ru-(TBP)(L)$_2$]. These observations show that from a spectroscopic point of view, the oligomer cannot be considered as made of independent chromophores. This is of course encouraging for our purpose as it suggests that extensive delocalization occurs in the oligomer. In the case of the pyrazine oligomer, the shape of the charge-transfer band was unusual, being very asymmetric (see Figure 4) and similar to the shape obtained by Taube et al. for pyrazine-bridged oligomers.[15]

Redox Potentials. Results of cyclic voltammetry experiments are summarized in Table II. The free porphyrin exhibits a

(13) Gouterman, M. In *The Porphyrins*; Dolphin, D., Ed.; Academic Press: New York, 1978; Vol. III, p 7.

(14) Gouterman, M. In *The Porphyrins*; Dolphin, D., Ed.; Academic Press: New York, 1978; Vol. III, p 112. Antipas, A.; Buchler, J. W.; Gouterman, M.; Smith, P. D. *J. Am. Chem. Soc.* **1978**, *100*, 3016.

(15) von Kameke, A.; Tom, G. M.; Taube, H. *Inorg. Chem.* **1978**, *17*, 1790.

Table II. Electrochemical Results in CH_2Cl_2, on a Platinum Wire Electrode[a]

compd	peak potentials, V vs SCE	
	cathodic	anodic
H_2TBP	−1.22*	+0.85, +0.95, +1.40, +1.55
[Ru(TBP)CO(EtOH)]	−1.25 (i.d.)	+0.83, +1.18, 1.70
$[Ru(TBP)(CH_3CN)_2]$		no defined peaks
$[Ru(TBP)(pyz)_2]$	−1.4 (i.d.)	+0.32* (Ru), +1.27
$[Ru(TBP)(azpy)_2]$	−0.88 (azpy)	+0.46* (Ru), +1.18
$[Ru(TBP)(pyz)]_n$	−1.4 (i.d.)	+0.57* (Ru), +1.30
$[Ru(TBP)(azpy)]_n$	−0.85 (azpy)	+0.67* (Ru)

[a] Ru: peak due to the ruthenium(II/III) couple. Azpy: peak due to coordinated 4,4′-azopyridine. i.d.: ill-defined peak. Asterisks designated reversible peaks (their anodic or cathodic counterpart observed in the return scan is not listed).

reduction peak at −1.22 V and several oxidation peaks (+0.85, +0.95, +1.4, and +1.55 V). Due to the conjugated character of the porphyrin ring, these peaks are attributed to population or depopulation of π^* and π levels, respectively. In the case of [Ru(TBP)CO], the oxidation peaks are in the same general range; no peak corresponding to ruthenium is observed, which is not surprising due to very strong stabilization of ruthenium(II) by the carbonyl ligand, which shifts the ruthenium(II/III) oxidation toward very high values. The reduction peak of the porphyrin becomes ill-defined but occurs in the same range as for free porphyrin. Curiously, $[Ru(TBP)(CH_3CN)_2]$ does not give identifiable peaks but only a smooth increase with respect to background current in both the anodic and cathodic explorations.

The monomeric and oligomeric complexes with pyrazine and azopyridine show the reversible anodic peak corresponding to the ruthenium(II/III) couple, plus the reduction peak of the axial ligand in the case of azopyridine. The cathodic peak of the porphyrin is absent, probably being shifted outside the working range. Similarly, the anodic features are also shifted, but in the opposite direction, so that the first one occurs near 1.2 V (see Table II). These changes seem to imply a strong interaction between π or π^* levels of the porphyrin and the ruthenium d orbitals.

For $[Ru(TBP)(azpy)_2]$, the cathodic wave at −0.88 V is attributed to the reduction of azopyridine to its monoradical anion, as for the ruthenium pentaammine complexes.[8] The ruthenium(II) oxidation appears at +0.46 V, which is a rather high value. This seems to be correlated with the number of azopyridine ligands linked to ruthenium. Since the ruthenium(II/III) system is reversible, it is easy to locate the standard potential from the classical figure formed by the anodic peak and its cathodic counterpart. One obtains here 0.41 V to be compared with −0.18 V for $[Ru(NH_3)_5H_2O]^{2+/3+}$ and +0.18 V for $[Ru(NH_3)_5(azpy)]^{2+/3+}$.[8] This trend can be easily rationalized by the influence of the π^* orbitals of azopyridine which stabilize preferentially ruthenium(II) and thus shift the standard potential of the ruthenium(II/III) couple toward positive potentials.

As for ruthenium pentaammine complexes of azopyridine,[8] the redox potentials show that, in the absence of protons, ruthenium(II)/azopyridine is a stable distribution of oxidation states, i.e. ruthenium(II) does not reduce azopyridine to its radical anion. However, in the presence of H^+ ions, one has to consider the 4,4′-azopyridine/1,2-bis(4-pyridyl)hydrazine couple, for which the apparent standard potential increases with acidity. This explains qualitatively that a crossing of potentials can occur, giving ruthenium(III)/bipyridylhydrazine as a stable state (see below). A more detailed investigation of the H^+ influence is not practicable here due to the difficulty to define the pH in CH_2Cl_2 or $CHCl_3$.

Intervalence Transitions. Progressive oxidation of the different complexes could be performed in chloroform, using titrated solutions of iodine as oxidant. Chloroform ensures a good solubility of the porphyrin complexes and above all a large spectral window, from 200 to 2400 nm. Special attention was paid to a possible oxidation of the OH groups of the porphyrin into quinone groups, but inspection of the UV–visible spectra, which are very sensitive to the porphyrin state,[11] showed no sign of such reaction.

Table III. Values of the Apparent Extinction Coefficients of the Intervalence Transitions[a]

compd	treatment	ϵ ($mol^{-1}\cdot L\cdot cm^{-1}$)
$[Ru(TBP)(pyz)]_n$	−0.5 e⁻/Ru	960
$[Ru(TBP)(azpy)]_n$	−0.5 e⁻/Ru	750
$[Ru(TBP)(bphy)]_n$	−0.5 e⁻/Ru	165
$[Ru(TBP)(azpy)]_n$	+0.5 H^+/Ru	620

[a] Bphy stands for 1,2-bis(4-pyridyl)hydrazine. The extinction coefficient is calculated at half-oxidation assuming that all the material is constituted by ruthenium(II)–ruthenium(III) pairs. No correction for the comproportionation equilibrium is performed.

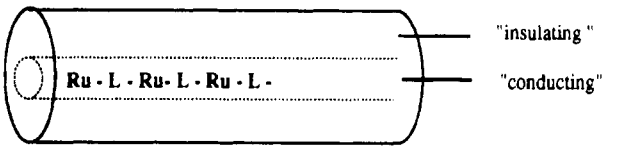

Figure 5. Topology of the pyrazine oligomer: an insulated wire.

Oxidation of the mononuclear complexes showed a simple decrease of the charge-transfer band which disappeared for 1 equiv of oxidant.

During the oxidation of the oligomers, the metal-to-axial-ligand charge-transfer band decreased continuously but not regularly. A broad band appeared in the near-infrared, which increased in intensity, passed through a maximum, and finally decreased. This is typical of an intervalence transition and compares well to the behavior described by Collman et al.[10] for porphyrin polymers bridged by pyrazine. This band can thus be used to probe the amount of electronic communication between redox sites in the oligomer.

With pyrazine as bridging ligand, the band maximum was estimated to be near 2400 nm (a more accurate location was impossible due to the solvent absorption). For comparison, in the case of octaethylporphyrin polymers bridged by pyrazine, Collman et al. obtained a band at 2900 nm.[10] It is remarkable that in analogous pyrazine-bridged oligomers where the metal sites were tetraammineruthenium, Taube[15] reported intervalence bands at markedly higher energies (ca. 8000 cm^{-1}, i.e. 1250 nm). Thus the porphyrin structure seems to confer low energies to the intervalence transitions, probably because it minimizes the structural rearrangements between the two redox sites and also because it shields these sites from the solvent influence.

Due to the difficulty to define a comproportionation constant here, we shall use systematically for comparison purposes the maximum apparent extinction coefficient at half-oxidation. It is obtained from the total concentration expressed in *dimeric* units, thus considering that the chromophore is the Ru(II)–Ru(III) pair. With this convention, the maximum apparent extinction coefficient was 960 $mol^{-1}\cdot L\cdot cm^{-1}$ (see Table III).

To conclude the case of the pyrazine oligomer, it is necessary to mention a strange behavior which occurred during oxidation: the amount of iodine necessary for a complete oxidation was found much greater (by a factor of at least 2) than could be calculated from stoichiometry, and the attainment of equilibrium was slow. No sign of a possible oxidation of the porphyrin was detected, and we attribute this behavior to the steric difficulty to reach the redox sites. Inspection of molecular models showed that, with this short ligand, the bulky porphyrins must adopt a staggered conformation which protects efficiently the metal–ligand spine from outside. In other words, this oligomer can be considered as an "insulated wire" (Figure 5).

In the case of the azopyridine oligomer, the behavior upon oxidation was more regular; i.e., the end point was observed very near to the theoretical stoichiometry and no slow evolution was observed. This is attributed to the fact that the longer azopyridine imparts a less crowded structure to the oligomer and thus favors

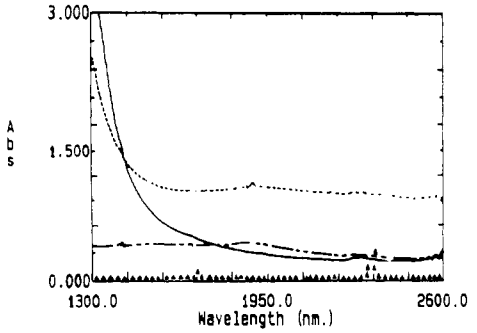

Figure 6. Oxidation of the $[Ru(TBP)(azpy)]_n$ oligomer in chloroform ($C = 2.8 \times 10^{-3}$ M in monomeric unit; 1-cm path length). Key: —, starting material; - - -, half-oxidized species; — -, fully oxidized species; ▲, base line corresponding to solvent alone.

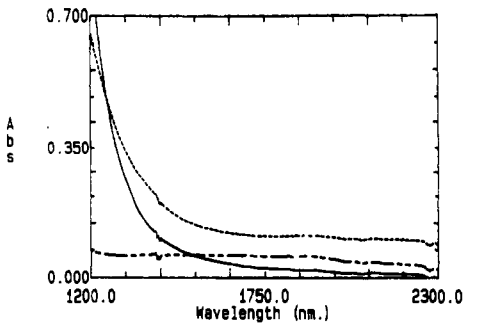

Figure 7. Switching "on" the intervalence transition on the $[Ru(TBP)(azpy)]_n$ oligomer in chloroform ($C = 3.4 \times 10^{-4}$ M in monomeric unit; 1-cm path length). Key: —, starting azopyridine oligomer; - - -, + 0.5 H^+ per Ru; — -, + 1 H^+ per Ru.

the access of the oxidant to the ruthenium sites. The intervalence band was observed here as a general increase of optical density between 1500 and 2600 nm without a discernible maximum (see Figure 6). The spectral evolution could be reversed by action of zinc amalgam, showing that the oxidation process was reversible. Thus here again, the intervalence transition occurs at a low energy (by contrast, in the case of the ruthenium pentaammine dimer, the intervalence band could not be resolved from the nearby charge-transfer band,[8] which is an indication of a rather high energy). The maximum apparent extinction coefficient was 750, only slightly less than with pyrazine (see Table III).

Influence of Protonation of $[Ru(TBP)(azpy)]_n$. If we perform an acid titration of the azopyridine oligomer in $CHCl_3$, a clear end point is observed for 1 H^+ per mononuclear unit. The ruthenium(II) to azopyridine charge-transfer band (960 nm in this medium) disappears, while a weak band appears at 538 nm, which is assigned to a ligand-to-ruthenium(III) transition. The Soret band is unchanged, showing that the porphyrin has not been involved. When a similar experiment is performed on the pyrazine oligomer, no spectral changes are observed. These results are consistent with the following reaction:

$$[Ru^{II}(TBP)\text{–}L]_n \xrightarrow{nH^+} [Ru^{III}(TBP)\text{–}LH_2\text{–}Ru^{III}(TBP)\text{–}L\text{–}Ru^{III}(TBP)\text{–}LH_2\text{–}Ru^{III}(TBP)\text{–}L\text{–}]_{n/4}$$

L = 4,4′-azopyridine
LH_2 = 1,2-bis(4-pyridyl)hydrazine

Indeed, due to the stoichiometry of the complex, there is not enough ruthenium(II) to reduce the totality of the ligand (cf. the case of the mononuclear pentaammine complex), so that the final compound contains azopyridine and 1,2-bis(4-pyridyl)hydrazine in equal quantities.

At half-acidification, i.e. when 0.5 H^+ has been added per monomeric unit, the oligomer must be in a mixed-valence state containing as much ruthenium(II) as ruthenium(III) and L and LH_2 in a ratio of three to one:

$$[Ru^{II}(TBP)\text{–}L]_n \xrightarrow{(n/2)H^+} [Ru^{II}(TBP)\text{–}LH_2\text{–}Ru^{III}(TBP)\text{–}L\text{–}Ru^{II}(TBP)\text{–}L\text{–}Ru^{III}(TBP)\text{–}L\text{–}]_{n/4}$$

(e⁻ transfers)

This gives the possibility to observe an intervalence transition between ruthenium(II) and -(III). This is effectively what occurs; i.e., the intervalence band is switched "on" by the proton addition (see Figure 7). Note that this intervalence transfer occurs most probably at the places where ruthenium(II) and -(III) are connected through the L form. If we compare the apparent extinction coefficients of the intervalence bands, we obtain 620 in the present case versus 750 for the normal mixed-valence oligomer obtained by the oxidation method (Table III). Thus

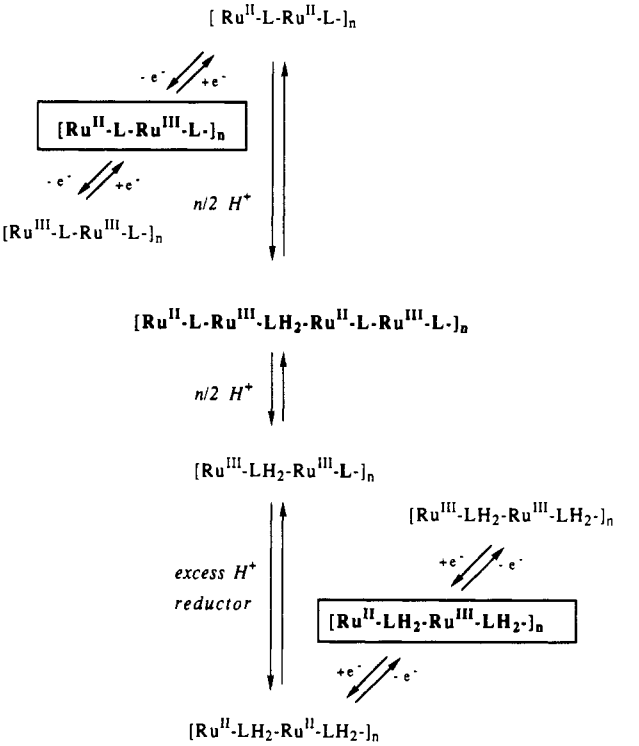

Figure 8. Final scheme showing the different species obtained from ruthenium porphyrin bridged by 4,4′-azopyridine.

the presence of one fourth of bridging ligand under the LH_2 form has no dramatic consequences.

It is also interesting to remark that this process is very analogous to the protonic doping process which has been observed in some conducting polymers[16] and also in conjugated molecular species.[17]

Thus, from the point of view of the ability of the oligomer to transfer electrons along the chain, the influence of protons is 2-fold: it generates ruthenium(III) from ruthenium(II), which gives a mixed-valence state (this is favorable), but at the same time it converts 4,4′-azopyridine into 1,2-bis(4-pyridyl)hydrazine, which is a priori unfavorable. To separate these two effects, we have investigated oligomer chains bridged by 1,2-bis(4-pyridyl)-hydrazine.

Treating the azopyridine oligomer by H^+ and then sodium borohydride (see Experimental Section) generates the fully reduced form in which ruthenium is in the (II) state and the ligand in the LH_2 state (see bottom of Figure 8). Subsequent redox titration by iodine gave a new intervalence transition, with a different profile than in the previous case; the band was narrower, so that a true maximum could be located at 1200 nm. This shows that the reduction bears on the ruthenium sites, thus generating a mixed-valence chain bridged by the reduced form of the ligand

(16) Han, C. C.; Elsenbaumer, R. L. *Synth. Met.* **1989**, *30*, 123.
(17) Spangler, C. W. Private communication, June 1990.

(Figure 8). The maximum apparent extinction coefficients was found to be 165 (Table III), showing that the electronic interaction has been strongly reduced with respect to the original structure but has not disappeared. This result is reminiscent of Haga's work,[6] in which the intervalence band was also modified but by a true protonation/deprotonation reaction.

Conclusion and Prospects

The ruthenium porphyrin oligomers described here present some interesting potentialities for molecular electronics. The first one is merely the "insulated wire" topology exhibited by the pyrazine oligomer, for which we are not aware of other examples. This could be a way to eliminate some drawbacks frequently encountered in conducting polymers: the high chemical reactivity giving parasitic reactions on the conjugated chains and the tendency for these conducting chains to aggregate, which precludes the experimental study of isolated chains. Another remarkable result is the successful identification of the metal-to-axial-ligand charge-transfer bands. This heralds the possibility to photochemically activate an electron transfer along the chain.

However, the most interesting result is the possibility to reproduce the basic process of H^+-induced redox reaction already encountered in the binuclear pentaammineruthenium complex. Thus H^+ ions can really be used to control an intramolecular electron-transfer process. But H^+ ions are introduced (or removed) here by a macroscopic experiment. In order to exploit this effect at the truly molecular scale, one has to devise a complex supramolecular assembly incorporating an activable proton generator or scavenger. Several possibilities exist, namely compounds which release protons by an electrochemical process or upon a photonic excitation (cf. the proton pumps encountered in biology).

Acknowledgment. The authors are indebted to Prof. J. Simon, ESPCI Paris, for his help in the starting of this research. Financial help of the Région Midi-Pyrénées (Contract No. 9000840 of Pôle Matériaux) is gratefully acknowledged.